Published in final edited form as:
J Proteome Res. 2012 April 6; 11(4): 2480–2491. doi:10.1021/pr201180m.

PROTEOMIC CHARACTERIZATION OF THE CELLULAR RESPONSE TO NITROSATIVE STRESS MEDIATED BY S-NITROSOGLUTATHIONE REDUCTASE INHIBITION

Matthew W. Foster[‡,1], **Zhonghui Yang**[‡,1], **David M. Gooden**[¶], **J. Will Thompson**[#], **Carol H. Ball**[§], **Meredith E. Turner**[#], **Yongyong Hou**[^], **Jingbo Pi**[^], **M. Arthur Moseley**[#], and **Loretta G. Que**[‡,2]

[‡]Division of Pulmonary, Allergy and Critical Care Medicine, Duke University Medical Center, Durham, NC 27710

[¶]Small Molecule Synthesis Facility, Duke University Medical Center, Durham, NC 27710

[#]Institute for Genome Sciences and Policy, Duke University Medical Center, Durham, NC 27710

[§]Agilent Technologies, Inc., Cary, NC 27758

[^]The Hamner Institute for Health Sciences, Research Triangle Park, NC 27709

Abstract

The S-nitrosoglutathione-metabolizing enzyme, GSNO reductase (GSNOR), has emerged as an important regulator of protein S-nitrosylation. GSNOR ablation is protective in models of asthma and heart failure, raising the idea that GSNOR inhibitors might hold therapeutic value. Here, we investigated the effects of a small molecule inhibitor of GSNOR (GSNORi) in mouse RAW 264.7 macrophages. We found that GSNORi increased protein S-nitrosylation in cytokine-stimulated cells, and we utilized stable isotope labeling of amino acids in cell culture (SILAC) to quantify the cellular response to this “nitrosative stress”. The expression of several cytokine-inducible immunodulators, including osteopontin, cyclooxygenase-2 and nitric oxide synthase isoform 2 (NOS2) were decreased by GSNORi. In addition, selective targets of the redox-regulated transcription factor, nuclear factor (erythroid-derived 2)-like 2 (Nrf2)—including heme oxygenase 1 (HO-1) and glutamate cysteine ligase modulatory subunit—were induced by GSNORi in a NOS2- and Nrf2-dependent manner. In cytokine-stimulated cells, Nrf2 protected from GSNORi-induced glutathione depletion and cytotoxicity, and HO-1 activity was required for downregulation of NOS2. Interestingly, GSNORi also affected a marked increase in NOS2 protein stability. Collectively, these data provide the most complete description of the global effects of GSNOR inhibition and demonstrate several important mechanisms for inducible response to GSNORi-mediated nitrosative stress.

Keywords

Nitric oxide; S-nitrosylation; S-nitrosoglutathione; GSNO reductase; proteomics; heme oxygenase

[2]To whom correspondence should be addressed. loretta.que@dm.duke.edu.
[1]These authors contributed equally

Supporting Information Available. Supporting information includes a description of the synthesis and characterization of the GSNOR inhibitor. In addition, Excel files for both the GeLC and GelFree datasets contain fold changes and p-values for each unique identified SILAC pair, as well as protein-level fold changes and p-values, # of quantified SILAC pairs and # of identified peptides per protein. A Scaffold file containing all identified MS/MS spectra and % sequence coverage for each identified protein, is available for download at https://proteomecommons.org using passphrase “GSNORi”.

INTRODUCTION

The biological effects of nitric oxide (NO) are mediated in significant part through the S-nitrosylation of low-mass and protein thiols to form S-nitrosothiols (SNOs)[1, 2]. S-nitrosoglutathione is a measurable product of NO synthase (NOS) activity[3], and the reversible transnitrosylation of protein thiol by GSNO (to form SNO-protein), as well as denitrosylation of SNO-protein by glutathione, have been long thought to govern the cellular homeostasis and speciation of SNOs. It is becoming increasingly evident that enzymes which catalyze denitrosylation of GSNO and SNO-proteins (e.g. GSNO reductase and thioredoxin, respectively) and their regulators (e.g. thioredoxin-interacting protein) are largely responsible for controlling cellular SNO homeostasis[4, 5].

Glutathione-dependent formaldehyde dehydrogenase (GS-FDH; GSNOR) was the first described GSNO reductase[6]; in the presence of excess GSH, the enzyme catalyzes the NADH-dependent reduction of GSNO to glutathione disulfide and ammonia[6, 7]. GSNOR is highly conserved across phylogeny and its deletion in *E. coli* and yeast results in increased protein S-nitrosylation and cytotoxicity in response to exogenous S-nitrosothiols and NO donors[7, 8]. GSNOR deletion also results in increased SNO-proteins and decreased survival in mice exposed to endotoxin, and these effects are attenuated by an inhibitor of nitric oxide synthase 2 (NOS2; iNOS)[9]. Subsequent investigations of the GSNOR knockout ($GSNOR^{-/-}$) mouse have shown that GSNOR deficiency promotes hepatocarcinoma (HCC)[10, 11] but protects from allergic asthma[12] and ischemic heart failure[13]; GSNOR deficiency is linked to S-nitrosylation of the DNA repair enzyme O(6)-alkylguanine-DNA alkyltransferase[10], the regulators of beta adrenergic receptor trafficking and signaling, GRK2 and beta-arrestin 2[14, 15], the transcription factor hypoxia inducible factor 1α[13] and the apoptotic effector glyceraldehyde 3-phosphate dehydrogenase (GAPDH)[16]. Collectively, studies of GSNOR have established an important role for the enzyme in signal transduction by nitric oxide and protection against “nitrosative stress”, the cytostatic or cytotoxic effects resulting from pathophysiological levels of protein S-nitrosylation. Still, relatively little is known about the scope and nature of GSNOR-regulated pathways.

Recently, Sanghani and coworkers reported the identification of three GSNOR-specific inhibitors via high-throughput screening of a 60,000 compound small-molecule library[17]. GSNOR inhibition was shown in RAW 264.7 mouse alveolar macrophages to potentiate GSNO-dependent S-nitrosylation and to inhibit nuclear factor kappa b (NF-κB) activation under conditions of constitutive NOS activity. RAW 264.7 cells are well-characterized in their ability to produce high levels of NOS2 and S-nitrosylated proteins in response to lipopolysaccharide (LPS) and murine interferon gamma (IFNγ)[18]. We reasoned that the quantification of GSNOR inhibitor-dependent protein expression under similar conditions would aid in elucidating GSNOR-regulated signaling pathways and the cellular response to nitrosative stress.

MATERIALS AND METHODS

Materials

Chemicals were purchased from Sigma-Aldrich unless otherwise noted. 4-[[2-[[(2-cyanophenyl)methyl]thio]-4-oxothieno[3,2-d]pyrimidin-3(4H)-yl]methyl]-benzoic acid (GSNORi) was synthesized by the Small Molecule Synthesis Facility at Duke University and characterized by NMR and ESI-MS (Supporting Information). Antibodies and dilutions were as follows: NOS2 (Millipore AB5382, 1:1000), GAPDH (Millipore 6C5, 1:3000), osteopontin (R&D Systems AF808, 1:1000), heme oxygenase 1 (Enzo ADI-SPA-895, 1:1000), ubiquitin (Cell Signaling #3933, 1:1000).

Cell culture

RAW 264.7 macrophages (ATCC) were cultured in Dulbecco's modified eagle medium (DMEM) unless otherwise noted. RAW 264.7 macrophages stably overexpressing scrambled- or Nrf2-shRNA were previously described[19, 20] and were cultured in DMEM containing 20 mM Hepes and 5 μg/ml puromycin.

Photolysis chemiluminescence

Mercury-coupled photolysis chemiluminescence was performed as described previously[21]. Low- and high-mass SNOs were isolated by centrifugal filtration of lysates using an Amicon Ultra-4 10 kDa centrifugal concentrator (Millipore), where the low-mass fraction represented the flow through and high-mass fraction was the retentate. Standard curves were generated using S-nitrosoglutathione, prepared by the method of Hart[22].

SILAC labeling and treatment of mouse macrophages

RAW 264.7 cells were cultured in SILAC DMEM (Pierce) supplemented with 10% dialyzed fetal bovine serum (Sigma), Pen/Strep/Fungizone (Gibco), 10 mg/l proline, and 50 mg/l arginine and lysine (light) or 50 mg/l $^{15}N_4{}^{13}C_6$-arginine and $^{15}N_2{}^{13}C_6$-lysine (heavy). Cells were conditioned in heavy DMEM for a minimum of 6 doublings. One 150 mm dish of either light or heavy isotope-labeled cells was treated with DMSO (light) or 50 μM GSNORi in DMSO (heavy) followed by addition of 500 ng/ml LPS and 10 ng/ml IFNγ (cytomix; CM). After 12 h, cells were washed with cold phosphate-buffered saline (PBS) and scraped in lysis buffer (PBS containing 0.5% NP-40 and Complete Protease Inhibitors (Roche)). After centrifugation at 20,000 × *g* for 10 min, protein was quantified by BCA assay (Pierce) and equal amounts of light and heavy-labeled lysates were mixed.

1D-SDS-PAGE-LC-MS/MS

50 μg of combined lysates were separated by SDS-PAGE on a 4–12% SDS-PAGE gel (Invitrogen NuPage). After staining with Colloidal Blue (Invitrogen), the protein lane was cut into 32 bands using a 2 mm × 7 mm gridcutter (GelCompany) and in-gel tryptic digestions were performed as previously described [23]. Finally, peptides were extracted with ddH_2O containing 1% formic acid (FA) and 2% acetonitrile (ACN) followed by 100% ACN, and extracts were transferred to Total Recovery LC Vials (Waters). After lyophilization, peptides were resuspended in 12 μl 0.2% FA, 2% ACN in ddH_2O.

Samples were analyzed by a nano-ESI-Chip system interfaced to a 6520 QTof (Agilent). The large-capacity Chip contained a 160 nl C18 trapping column and a 0.75 × 150 mm 300 Å C18 analytical column. Five μl of tryptic digests were first trapped at 3.5 μl/min and were separated on the analytical column at 300 nl/min using a linear gradient of 5–40% ACN containing 0.1% FA over 50 min. Samples were analyzed by data-dependent analysis (DDA) with MS scans acquired at 4 scans/s from 300–1800 Da and MS/MS scans at 2 scans/s from 59–2000 Da. The top 5 most intense ions were selected for MS/MS analysis and each precursor ion was excluded after 1 scan and released after 0.4 min. Precursor ion selection was based on abundance and charge state with doubly and triply charged ions preferred. Collision energy (CE) followed a linear equation of CE = (3.6 V per 100 Daltons) − 4.6V.

GelFree-LC-MS/MS

1 mg of combined lysates was exchanged against 50 mM ammonium bicarbonate and concentrated to 100 μl using a 10 kDa cutoff 0.5-Ultrafree centrifugal concentrator (Millipore). The sample was brought up to 150 μl with 30 μl of 5x acetate sample buffer (Protein Discovery), 8 μl of 1M DTT and remainder ddH2O and was heated at 50 °C for 10

min. The sample was separated into 12 fractions using a GelFree8100 Fractionation System (Protein Discovery) with an 8% Tris-Acetate Cartridge according to the manufacturer's protocol. Following separation, detergent removal columns (Pierce) were used for SDS removal. A total of 10 μg protein from each fraction was resuspended in 0.1% w/v Rapigest SF (Waters), reduced with 10 mM, alkylated with 20 mM iodoacetamide, and digested o/n at 37 °C with 1:50 trypsin.

Peptide digests from each GelFree fractions were analyzed using a nanoAcquity UPLC system coupled to a Synapt G1 HDMS mass spectrometer (Waters). Approximately 1 μg digest was trapped on a 20 μm × 180 mm Symmetry C18 column (Waters) at 20 μl/min for 2 minutes in water containing 0.1% FA, and further separated on a 75 μm × 250 mm column with 1.7 μm C18 BEH particles (Waters) using a gradient of 5 to 40% ACN/0.1% FA over 90 min at a flow rate of 0.3 μl/min and a column temp of 45 °C. Samples were analyzed twice in data-dependent (DDA) mode and once in data-independent (MS^E) mode. DDA used a 0.9 s precursor scan followed by MS/MS product ion scans from on the top 5 most intense ions using a dynamic exclusion window of 120 s. MS^E runs used 0.9 s cycle time alternating between low collision energy (6 V) and high collision energy ramp (15 to 40 V).

Peptide identification and SILAC quantification

Quantification was performing using Rosetta Elucidator v3.2 (Rosetta Biosoftware), and peptide/protein identifications were made with Mascot v2.2 (Matrix Sciences) or Protein Lynx Global Server v 2.4 (PLGS; Waters) for data-dependent and MS^E acquisitions, respectively. Searches were performed against the SwissProt database v57.1, with mouse taxonomy and containing a reverse decoy database. Mascot search parameters were 10 ppm or 20 ppm precursor (for Agilent and Waters data, respectively) and 0.04 Da product ion tolerance, with oxidized (M), deamidation (NQ), Label:$^{13}C_6{}^{15}N_2$ (K) and Label:$^{13}C_6{}^{15}N_4$ (R) as variable modifications. MS^E data was searched in PLGS without heavy K and R modifications. Peptide identifications were accepted if they had a <1% FDR as determined with the PeptideTeller algorithm in Elucidator[24, 25]. A supplemental dataset, "GSNORi_MSMS" containing all assigned MS/MS spectra is available for download at https://proteomecommons.org using passphrase "GSNORi". The file "GSNORi_MSMS.sf3" can be viewed using the Scaffold Free Viewer (Proteome Software).

SILAC pairs (light and heavy Arg- and/or Lys-containing forms of the same peptide) were located in Elucidator with a minimum *m*/*z* tolerance of 30 ppm and retention time tolerance of 0.2 min and a maximum of three labeled amino acids per peptide. However, to simplify the analysis, peptides that were confidently identified but did not have an associated pair were not quantified; this would exclude peptides to keratins and other contaminants (e.g. bovine serum albumin) as well as peptides at the extreme C-termini of proteins, which do not contain K or R. The SILAC ratios were calculated in Elucidator using the highest abundance member of each isotope cluster, with intensity normalization enabled for global correction of bias in mixing between heavy and light lysates. P values were calculated according to an error model as previously described[26, 27].

High-confidence quantifications were based on the H/L peak height ratios of 2 or more unique SILAC pairs for a given protein. SILAC pairs with identical modified peptide sequences but different charge states were counted as a single pair. However, pairs which contained identical peptide sequences but differed by a post-translation modification (e.g. Met oxidation) were counted as unique. For the purpose of counting number of peptides sequenced per protein, a peptide identified with multiple charge states (e.g. 2^+, 3^+) was counted once, and different modified forms of the same peptide (including heavy forms) were each counted as unique identifications.

Real-time PCR

Total RNA was isolated from Raw 264.7 cells with TRIzol (Invitrogen) and Qiagen RNeasy Mini Kit according to manufacturers' instructions. A total of one microgram of RNA was used for reverse transcription using the High Capacity cDNA Reverse Transcription Kit (Applied Biosystems). Real-Time PCR was performed in a Bio-Rad iCycler using SYBR green reagent (Bio-Rad, Hercules) under standard conditions. Primer sequences were as following: Actin: 5′-TCA AGA TCA TTG CTC CTC CTG-3′ (for), 5′-CTG CTT GCT GAT CCA CAT CTG-3′ (rev); BlvbR: 5′-TCC TCG GAG TTC TCA GCT TT-3′ (for), 5′-GCA CCG TCA CCT CAT AAC CT-3′ (rev); COX-2: 5′-CTG CAG AAT TGA AAG CCC TC-3′ (for), 5′-TTC CAG TAT TGA GGA GAA CAG-3′ (rev); GCLM: 5′-GCC ACC AGA TTT GAC TGC CT-3′ (for), 5′-AGG GAT GCT TTC TTG AAG AG-3′ (rev); HO-1: 5′-CAC GCA TAT ACC CGC TAC CT-3′ (for), 5′-CCA GAG TGT TCA TTC GAG CA-3′ (rev); Nrf2: 5′-CGA GAT ATA CGC AGG AGA GGT AAG A-3′ (for), 5′-GCT CGA CAA TGT TCT CCA GCT T-3′ (rev); NOS2: 5′-TGG CTA CCA CAT TGA AGA A-3′ (for), 5′-GAC TGT AGG GAC GAT TGG AG-3′ (rev); RSAD2: 5′-TGT TCC CCT TGA GAA ACT GG-3′ (for), 5′-TAT TCC AAA GCA GAA AAGC-3′ (rev).

Relative quantification was performed using comparative threshold C_T analysis. Gene expression cycle changes were expressed as fold change using actin as internal control.

Assay of total intracellular glutathione (GSH)

Cells were sonicated in cold PBS immediately after collection followed by centrifugation at 12,000 × *g* for 5 min. The resulting supernatants were used for measurement of total GSH using BIOXYTECH GSH/GSSG-412 kit (OxisResearch) as previously described[28].

Lactate dehydrogenase (LDH) assay

LDH in cell culture supernatants was quantified by the LDH Cytotoxicity Assay Kit (Cayman) according to the manufacturer's instructions. Standard curves were generated using purified LDH.

RESULTS

A GSNOR inhibitor potentiates NOS2-dependent protein S-nitrosylation

Based on previous studies of GSNOR$^{-/-}$ mice, we hypothesized that NOS2-derived S-nitrosylation would be significantly potentiated by pharmacological GSNOR inhibition. RAW 264.7 macrophages were treated with or without a mixture of lipopolysaccharide and interferon gamma (cytomix; CM) to induce NOS2, and NO-derived species were quantified after simultaneous treatment of cells with or without the GSNOR inhibitor, 4-[[2-[[(2-cyanophenyl)methyl]thio]-4-oxothieno[3,2-d]pyrimidin-3(4H)-yl]methyl]-benzoic acid (GSNORi)[17]. Lysates were separated into high- and low-mass fractions by centrifugal filtration, and mercury-displaceable (i.e. SNO) and non-labile NO species (XNO; e.g. Fe-NO, N-NO)[8] were measured by photolysis chemiluminescence. Low-mass species (e.g. GSNO) were below detectable limits across all conditions (data not shown), and high-mass NO congeners were also undetected in unstimulated cells (Fig. 1A). In CM-stimulated cells, GSNORi caused a >3-fold increase in high-mass protein S-nitrosothiols, which is comparable to the increase observed in livers from GSNOR$^{-/-}$ versus WT mice following intraperitoneal injection of LPS[9]. However, protein-XNO species were only modestly increased (Fig. 1A). The specific modulation of protein-SNO levels (but not protein-XNO) by GSNOR was consistent with observations in the GSNOR$^{-/-}$ mouse and in a yeast model of nitrosative stress[8, 9].

We also quantified levels of the NO metabolite, nitrite, in culture media. Nitrite was only detectable by Griess assay after cytokine stimulation (Fig. 1B), and interestingly, nitrite levels were lower after GSNORi treatment, possibly due to a shift in the cellular equilibrium between NO and GSNO, or alternatively, SNO-dependent effects on NOS2 activity or expression [29, 30]. Indeed, we observed a decrease in NOS2 expression by GSNORi in stimulated cells (Fig. 1C).

Quantitative proteomic analysis of GSNORi-regulated proteins in cytokine-stimulated mouse RAW 264.7 macrophages

We hypothesized that the effects of GSNORi would be sensitively reflected in alterations to protein expression. To this end, we performed SILAC-based quantitative proteomics on CM-stimulated RAW 264.7 cells treated with or without GSNORi (Fig. 2A). Equal amounts of light and heavy lysates were mixed and separated first by 1D-SDS-PAGE, and thirty-two gel bands were excised, in-gel digested with trypsin and subjected to LC-MS/MS analysis (i.e. “GeLC analysis”; Fig. 2A). To exploit the reported benefits of multiple parallel separations, the lysate mixture was also subjected to GelFree fractionation[31], and twelve fractions were recovered. Following detergent cleanup, proteins were digested in solution with trypsin and analyzed by LC-MS/MS.

After processing of the data with Rosetta Elucidator, we selected proteins with two or more unique SILAC pairs as a criterion for confident quantification (see Methods). These totaled 807 and 707 proteins for GeLC and GelFree analyses, respectively (Supporting Information). Cumulatively, 987 unique proteins were confidently quantified, included 280 proteins that were unique to the GeLC analysis, 180 that were unique to the GelFree analysis and 527 proteins common to both datasets (Fig. 2B). We quantified 27 proteins that were induced at least 1.25-fold with GSNORi treatment ($p<0.0001$; Table 1 and Supporting Information) as well as 85 proteins that were downregulated >1.25-fold after GSNORi treatment ($p<0.0001$; Table 2 and Supporting Information). Proteins quantified by GeLC and GelFree approaches had very similar expression values (Table 1–2; Supporting Information). However, among the GSNORi-regulated proteins, osteopontin (OPN), which was the most downregulated, and glutamate cysteine ligase modulatory subunit (GCLM), which was ~2-fold upregulated, were only quantified by GelFree analysis. On the other hand, despite a reported separation range of 3.5–150 kDa for the GelFree cartridge, we quantified relatively few proteins above ~110 kDa with this method (Supporting Information). This phenomenon was apparent for NOS2 (133 kDa), which was quantified by 43 SILAC pairs by GeLC but only 2 SILAC pairs by GelFree analysis (Table 1–2; Supporting Information). Interestingly, the Moloney murine leukemia virus (MMLV) envelope glycoprotein was also among the most downregulated proteins (Table 2). It has been noted previously the RAW264.7 cells produce detectable levels of MMLV[32].

Heme oxygenase 1 (HO-1), glyceraldehyde 3-phosphate dehydrogenase (GAPDH) and NOS2 were found to be >4-fold induced, unchanged and ~2-fold downregulated by GSNORi, respectively. As a demonstration of the quantitative robustness of our workflow, we observed a strict correlation between these observed fold changes and the calculated H/L isotope intensities for each of the SILAC pairs associated with these proteins (Fig. 3A). However, we also considered the scenario where multiple MW forms of the same protein (due to alternative splicing, alternative translational initiation, or post-translational modification) might be differentially regulated by GSNORi. Although MW information (in the form of fraction or gel-band number; Supporting Information) was preserved in both analyses, GeLC had the higher resolution and we noted this phenomenon for several proteins. One example was the LPS-inducible protein, interleukin-1 receptor antagonist (IL-1Ra), which was quantified in two contiguous bands. We observed an overall 1.3-fold decrease in IL-1Ra for six quantified SILAC pairs; however, IL-1Ra was 2.5-fold lower in

the higher MW band (2 SILAC pairs) and essentially unchanged in the lower band (4 SILAC pairs; Fig. 3B). Cytokine-stimulated RAW 264.7 cells express two intracellular forms of 16 of 18 kDa by alternative translation initiation[33], and these data suggest that GSNORi may attenuate translation of the higher MW form. Ubiquitin was also unchanged in the lowest MW bands which most likely corresponded to free ubiquitin (−1.2 fold; 6 total SILAC pairs), whereas it was on average 1.8-fold lower in the ten highest MW bands (16 total SILAC pairs; Fig. 3B), suggestive of inhibition of protein ubiquitination machinery (e.g. E3 ligases[34, 35]) by S-nitrosylation. As we have also shown recently for differential protein SUMOylation[36], the potential for quantifying multiple forms of a protein is a potential advantage that GeLC and other protein MW-based separations may have over shotgun methods which separate proteomes only at the peptide-level.

As an initial validation of our quantitative analysis, we confirmed the GSNORi-dependent changes in expression of HO-1, GAPDH, NOS2 and OPN (Fig. 3C), and we also verified that protein ubiquitination was attenuated by GSNORi whereas low-mass ubiquitin appeared to be unchanged (Fig. 3D).

GSNORi targets potential nitrosative stress resistance proteins and immunomodulators

We next sought to identify common pathways affected by GSNOR inhibition. The inducible heme oxygenase, HO-1, the rate-limiting enzyme in heme degradation and a potent immunomodulator[37], was the most highly upregulated protein that met significance criteria (Table 1); by comparison, the constitutive heme oxygenase (HO-2) was unchanged. The induction of HO-1 by endogenous NOS and exogenous (S)NO is well characterized[38–42], and several mediators of (S)NO-dependent HO-1 induction have been previously identified, most notably the transcription factor nuclear factor (erythroid-derived 2)-like 2 (NFE2L2/Nrf2)[41–43]. A number of other Nrf2-dependent gene products were among the GSNORi-inducible proteome, including glutamate cysteine ligase regulatory subunit (GCLM), flavin reductase (biliverdin b reductase; BlvrB), aldose-reductase like protein 2, S-formylglutathione reductase and peroxiredoxin 1 (Table 1 and Supporting Information). However, many other classical Nrf2-inducible proteins, including additional heme detoxifying (biliverdin a reductase, ferritin light and heavy chains) and antioxidant proteins (e.g. catalase and glutathione reductase) were unchanged. Collectively, these data suggest GSNORi mounts a specific, rather than generic, stress response through Nrf2.

We hypothesized that an inducible response to nitrosative stress might in part explain the upregulation of proteins in response to GSNOR inhibition. Indeed, HO-1 has been shown to protect cells from the cytotoxic effects of NO[38, 39]. In addition, upregulation of GCLM would be expected to potentiate glutathione synthesis and promote protein denitrosylation. It is also interesting that S-formylglutathione hydrolase (immediately downstream of GSNOR in formaldehyde detoxification), lactoylglutathione lyase (glyoxylase), aldehyde and aldose reductases, and lens epithelial-derived growth factor (a stress-response transcription factor that regulates alcohol and aldehyde dehydrogenase genes[44, 45]) were also upregulated (Table 1 and Supporting Information). These changes might reflect an increase in formaldehyde stress due to GSNOR inhibition, or possibly indicate additional overlap (besides GSNOR and carbonyl reductase[46]) between proteins that regulate SNO and aldehyde clearance. As evidence of the latter, genetic deletion of S-formylglutathione hydrolase (esterase D) has been shown to render *N. gonnorrhoeae* sensitive to cell killing by GSNO[47].

As exemplified by the repression of NOS2 and OPN expression, cytokine-inducible proteins were also prominent among GSNORi-regulated proteins. Additional GSNORi-downregulated proteins included prostaglandin G/H synthase 2 (COX-2), radical S-adenosyl methionine domain-containing protein 2 (RSAD2) and uridine phosphorylase 1 (Table 2). This global phenomenon was not unexpected given that both exogenous S-nitrosothiols and

NOS2-derived NO have been shown to have mostly anti-inflammatory properties in cell and animal models[2]. On the other hand, a handful of cytokine-induced proteins were upregulated by GSNORi. It was surprising to find that GSNORi induced expression of the proinflammatory protein, intercellular adhesion molecule 1 (ICAM-1; Table 1) by >1.5-fold, since exogenous SNOs mostly been shown to suppress ICAM-1 expression. We also observed increased expression of the guanylate-binding proteins GBP1, GBP4 and GBP5. These coordinately-regulated GBPs are among the most highly induced genes in response to cytokine stimulation in RAW 264.7 cells[48, 49] and may have anti-inflammatory properties[50, 51]. An Ingenuity Pathway Analysis (not shown) did not reveal any common upstream activators (e.g. interferon regulatory factor 7) that might explain the specific induction of these GBPs versus other interferon-inducible genes that were either downregulated (e.g. interferon-induced protein 44-like) or unchanged (e.g. interferon-inducible GTPase 1) with GSNORi treatment.

GSNORi regulates gene transcription with a requirement for NOS2 activity

Based on their putative regulation by Nrf2, we hypothesized that mRNA levels of HO-1, GCLM and BlvrB expression would be increased by GSNORi, and we sought to determine whether NOS2 would be required for these effects Indeed, GSNORi greatly increased CM-dependent expression of all three genes, and the magnitude of these responses roughly paralleled the effects on protein-levels, with HO-1 exhibiting the largest fold-increase at the mRNA and protein levels (Fig. 4A and Table 1). Importantly, the NOS2-specific inhibitor 1400W reversed the effects of GSNORi, which suggested that the modulation of gene expression was due to an increase in NOS2-derived GSNO and not related to the formaldehyde-detoxifying activity of GSNOR. The abrogation of GSNORi- and CM-inducible HO-1 expression by NOS2 inhibitor was also confirmed by western blotting (Fig. 4B). At the same time, NOS2 expression in CM-stimulated cells was sensitive to 1400W at baseline and after GSNORi treatment (Fig. 4B), demonstrating a direct role for NOS activity in the downregulation of NOS2 by GSNORi.

Nrf2 is an effector of GSNORi-regulated gene expression and protects cells from nitrosative stress

We next sought to determine whether Nrf2 was critical for the induction of HO-1, GCLM and BlvrB by GSNORi and thus compared the effects of GSNORi on CM-induced expression of these genes in RAW 264.7 cells stably expressing a scrambled versus Nrf2-directed shRNA[20]. Basal Nrf2 expression was >80% reduced (Supporting Information) and the actin-normalized mRNA levels of all three target genes were lower after CM/GSNORi treatment in cells stably expressing Nrf2 versus scrambled shRNA (Fig. 5A). We investigated the effects of Nrf2 knockdown on the modulation of cellular GSH levels by CM and GSNORi. CM increased GSH levels ~2.5-fold in RAW 264.7 cells overexpressing scrambled shRNA, whereas there was a ~50% reduction in constitutive and CM-induced GSH levels in cells overexpressing Nrf2 shRNA (Fig. 5B). Despite the increase in GCLM mRNA in scrambled shRNA-overexpressing cells, we did not observe a significant change in GSH after GSNORi treatment. However, in Nrf2-deficient cells, GSNORi decreased GSH levels by ~30% in CM-stimulated cells versus CM alone. Thus, it appears that Nrf2 is important for GSH homeostasis under conditions of nitrosative stress. We further examined lactate dehydrogenase (LDH) levels in culture media under these conditions as a marker of cytotoxicity. While LDH was essentially unchanged in cells expressing scrambled shRNA, it was significantly higher in the CM- and GSNORi-treated cells as compared to CM alone (Fig. 5C). Collectively, these results suggest that Nrf2 is important for GSNORi-mediated gene expression and for maintenance of normal cellular redox status and protection from cytotoxicity during prolonged nitrosative stress.

Mechanism of GSNORi-dependent downregulation of NOS2

Our results demonstrated that NOS2 activity was required for the downregulation of NOS2 protein by GSNORi (Fig. 4B), and, we sought to further investigate the mechanism for this phenomenon that we hypothesized could represent an additional adaptive response to nitrosative stress. Besides a possible link between HO-1 and NOS2 (see discussion below), the overall decrease in expression of cytokine-inducible proteins suggested that SNO-dependent inhibition of a master transcription factor (e.g. NF-κB) might be responsible. Indeed S-nitrosylation of NF-κB p65 has been implicated in the feedback inhibition of NOS2 protein expression[30]. Other proteomic data was equivocal, as both the expression of ELAV1/HuR, which binds to the 3′-UTR of NOS2 and positively regulates cytokine-induced NOS2 expression[52] and hnRNP-L, a negative regulator of NOS2 expression[53], were lower with GSNORi.

In order to identify a mechanism, we first examined the levels of NOS2 mRNA under conditions where we observed downregulation of NOS2 protein (Fig. 4B). While GSNORi reduced NOS2 expression, 1400W did not reverse these effects and in fact, NOS2 inhibition reduced NOS2 mRNA under these conditions (Fig. 6A). Therefore, unlike HO-1 and related genes (Fig. 4A), NOS2 protein and mRNA did not strictly parallel each other at this time point. We were also unable to show an increase in S-nitrosylated NF-κB p65 under these conditions (not shown).

Based on previous reports that HO-1 and NOS2 expression and activity are inversely correlated in RAW 246.7 cells[54–57], we further sought to determine whether HO-1 might be important for downregulation of NOS2 by GSNORi. Co-incubation of RAW 246.7 cells with tin protoporphyrin IX (Sn-PP), a heme oxygenase inhibitor, increased nitrite production and reversed inhibition of NOS2 expression by GSNORi (Fig. 6B). Thus, HO-1 appears to have a principal role in GSNORi-dependent NOS2 downregulation, although additional mechanisms may also contribute to the inhibition of NOS2 activity.

Finally, we also examined the possibility that GSNORi might affect NOS2 levels via its ubiquitination or proteasomal degradation. We precipitated ubiquitinated proteins from cell lysates using a polyubiquitin-binding resin (TUBE1-agarose) and blotted for levels of NOS2 in whole cell lysates and in TUBE1-agarose precipitates (Fig. 6C). TUBE1 pulldowns were enriched for higher-MW forms of NOS2, indicative of Ubi-NOS2, and GSNORi appeared to decrease Ubi-NOS2 to a greater degree than total NOS2. These data were consistent with the observed decline in protein ubiquitination (Fig. 3B-C). We also examined the decline in NOS2 in CM- and GSNORi/CM-treated cells after inhibition of protein synthesis by cyclohexamide (CHX). In cells treated with cytomix alone, NOS2 protein was relatively stable for ~2 h following addition of CHX, whereas NOS2 levels declined sharply thereafter (Fig. 6D). Interestingly, while the initial level of NOS2 was lower in RAW 264.7 cells treated with both CM and GSNORi, NOS2 did not exhibit a measurable decline in these cells over the same time course (Fig. 6D). Collectively, these data suggest that GSNORi impairs NOS2 ubiquitination and degradation independently of effects on protein expression.

DISCUSSION

Despite an increasing appreciation of the (patho)physiological effects of aberrant GSNOR activity, a large gap still exists in our understanding of the importance of GSNO/GSNOR in signal transduction by nitric oxide. As compared to genetic tools such as the $GSNOR^{-/-}$ mouse, newly discovered GSNOR inhibitors[17, 58, 59] should enable the investigation of S-nitrosylation-based signaling in a wider variety of biological contexts. More importantly, these compounds also have potential utility as therapeutics in pulmonary and cardiovascular

diseases[12, 13], and thus there is a growing need to assess their global effects. In the past, mass spectrometry-based studies of S-nitrosylation have focused almost exclusively on the de novo identification of SNO-proteins and sites of S-nitrosylation. However, the enormity of proteomic data has not yielded an equivalent amount of biological insight, in part because the structural and functional significance of most of these modifications cannot be easily determined. S-nitrosylation has been shown to alter the expression of select proteins in RAW 264.7 cells, including HO-1 and thioredoxin-interacting protein (TXNIP)[5], and we hypothesized that an analysis of protein expression might be a more tractable approach to interrogate the effects of chronic GSNOR inhibition. Indeed, under our experimental conditions, GSNORi-dependent changes in the RAW 264.7 proteome appear to sensitively and specifically reflect both the anti-inflammatory actions of endogenous S-nitrosothiols and the cellular response to nitrosative stress. Nevertheless, our present study leaves open the question of the identity and functional significance of the S-nitrosoproteins that are targets of GSNORi. Future proteomic studies will focus on the mass spectrometry-based identification and quantification the Cys thiols that are modified by GSNOR inhibition in the cytokine-stimulated macrophage, with the goal of connecting these post-translational modifications to GSNORi-dependent signal transduction.

HO-1 has long been shown to be induced by exogenous S-nitrosothiols and by NOS2, with its expression being glutathione-dependent[60, 61] but cGMP-independent[38, 60]. Although these data have suggested that endogenous S-nitrosothiols affect HO-1 expression, we now provide definite proof that GSNO is an important regulator of HO-1 levels under conditions of high NO output, and this appears to hold true for GCLM, BlvrB and NOS2 as well. Although it is tempting to try and ascribe these phenomena to single regulatory events (e.g. activation of Nrf2), the mechanisms underlying SNO-dependent regulation of many of these proteins are likely multifactorial. Indeed, although Nrf2 appears to be play a role in GSNORi-dependent HO-1 expression, and modulators of Nrf2 stability and compartmentalization (Keap1 and Crm1, respectively) are targets of regulatory S-nitrosylation[43, 62], Nrf2 knockdown did not have measurably different levels of HO-1 following GSNORi/CM treatment (data not shown). This is consistent with the idea that additional mechanisms—including NO-induced stabilization of HO-1 mRNA by the mRNA-binding protein HuR[63], or activation of protein kinase C, MAP kinases and phosphatidylinositol 3-kinase[64–66]—may be important for induction of HO-1. Likewise, HO-1 appeared to fully restore NOS2 protein expression but did not fully restore activity; this may be related to timing of NOS2 versus HO-1 expression or may be evidence of post-translational regulation (e.g. S-nitrosylation) of NOS2 itself. The inhibition of NOS2 ubiquitination and degradation that we observe is also an intriguing and previously unappreciated consequence of nitrosative stress. While several E3 ubiquitin ligase complexes have now been shown to ubiquitinate NOS2 in RAW 264.7 cells[67–69], they were not quantified in our proteomic analysis, and further work is needed to determine how S-nitrosylation alters this important pathway for NOS2 clearance. More generally, the effects of GSNORi on high-MW ubiquitin indicate that control of protein ubiquitination machinery by S-nitrosylation extends beyond the few characterized targets[34, 35, 70].

The RAW 264.7 macrophage has long been a model of NOS2-based host defense and signaling, and how these cells cope with extraordinarily high levels of NOS2 activity has been an open question. Prior studies have identified multiple mechanisms for feedback inhibition of S-nitrosylation in CM-stimulated RAW 264.7 cells. For example, NOS2 protein expression is repressed in an NO dependent manner coinciding with S-nitrosylation of NF-κB[30], and the thioredoxin (Trx) inhibitor TXNIP is downregulated in RAW 264.7 cells by NOS2-derived NO[5], leading to activation of Trx-mediated denitrosylation. For the first time, our data shows that GSNOR has an important constitutive role in SNO-protein homeostasis in RAW 264.7 cells and that GSNOR inhibition can induce additional response

pathways. The induction of HO-1 appears to be important for downregulation of NOS2 protein and activity, with this and other potential protective effects possibly being mediated via products of heme catabolism (e.g. carbon monoxide, biliverdin). In addition, Nrf2 also appears to be a central mediator of protection from GSNORi-mediated glutathione depletion and cell death. Finally, the abundance of aldehyde-metabolizing and related enzymes among the GSNORi-induced proteins is suggestive of potential novel SNO-metabolizing enzymes. However, it should also be noted that NOS2 induces peroxiredoxins and sulfiredoxin in primary mouse macrophages[71], suggesting that there is potential crosstalk between responses to nitrosative stress and other stresses (e.g. reactive oxygen species) in these cells.

Although we demonstrate robust effects of GSNORi on protein S-nitrosylation and protein expression under a setting of high NOS2 expression, the most sensitive analytic tool at our disposable (photolysis-chemiluminescence) failed to detect an increase in SNOs in unstimulated cells, and similarly, GSNORi had no effect on expression of HO-1 (the most sensitive response indicator of S-nitrosylation) in the absence of NOS2. These findings are contrasted with those Sanghani et al. [17], who reported an increase in IKKβ S-nitrosylation and attenuation of TNFα-mediated phosphorylation of IKKβ by GSNORi in unstimulated RAW 264.7 cells, but did not fully evaluate the NOS-dependence of these effects. RAW 264.7 cells express constitutive eNOS (NOS3)[72], which unlike NOS2, requires activation via calcium-calmodulin or phosphorylation, so it is possible that GSNOR may modulate NO-dependent signaling during transient NOS3 activation. Nonetheless, our data support a model in which a critical threshold of NOS activity is required for GSNOR inhibition (or changes in GSNOR expression) to alter S-nitrosylation or SNO-mediated signaling. We predict that cells or tissues expressing high levels of constitutive or inducible NOS activity (e.g. endothelial and inflammatory cells) will be most susceptible to pharmacological GSNOR inhibition, and in turn, the extent to which these cells can limit the nitrosative stress due to GSNOR inhibition or deficiency is likely to impact the effectiveness of GSNOR inhibitor-based therapies.

Supplementary Material

Refer to Web version on PubMed Central for supplementary material.

Acknowledgments

This work was supported in part by the National Institutes of Health (HL086887 to L.G. Que) and (HL106121 to M.W. Foster) and through an instrument loan by Agilent Technologies.

References

1. Hess DT, Matsumoto A, Kim SO, Marshall HE, Stamler JS. Protein S-nitrosylation: purview and parameters. Nat Rev Mol Cell Biol. 2005; 6(2):150–66. [PubMed: 15688001]
2. Foster MW, Hess DT, Stamler JS. Protein S-nitrosylation in health and disease: a current perspective. Trends Mol Med. 2009; 15(9):391–404. [PubMed: 19726230]
3. Mayer B, Pfeiffer S, Schrammel A, Koesling D, Schmidt K, Brunner F. A new pathway of nitric oxide/cyclic GMP signaling involving S-nitrosoglutathione. J Biol Chem. 1998; 273(6):3264–70. [PubMed: 9452441]
4. Benhar M, Forrester MT, Stamler JS. Protein denitrosylation: enzymatic mechanisms and cellular functions. Nat Rev Mol Cell Biol. 2009; 10(10):721–32. [PubMed: 19738628]
5. Forrester MT, Seth D, Hausladen A, Eyler CE, Foster MW, Matsumoto A, Benhar M, Marshall HE, Stamler JS. Thioredoxin-interacting protein (Txnip) is a feedback regulator of S-nitrosylation. J Biol Chem. 2009; 284(52):36160–6. [PubMed: 19847012]
6. Jensen DE, Belka GK, Du Bois GC. S-Nitrosoglutathione is a substrate for rat alcohol dehydrogenase class III isoenzyme. Biochem J. 1998; 331 (Pt 2):659–68. [PubMed: 9531510]

7. Liu L, Hausladen A, Zeng M, Que L, Heitman J, Stamler JS. A metabolic enzyme for S-nitrosothiol conserved from bacteria to humans. Nature. 2001; 410(6827):490–4. [PubMed: 11260719]
8. Foster MW, Liu L, Zeng M, Hess DT, Stamler JS. A genetic analysis of nitrosative stress. Biochemistry. 2009; 48(4):792–9. [PubMed: 19138101]
9. Liu L, Yan Y, Zeng M, Zhang J, Hanes MA, Ahearn G, McMahon TJ, Dickfeld T, Marshall HE, Que LG, Stamler JS. Essential roles of S-nitrosothiols in vascular homeostasis and endotoxic shock. Cell. 2004; 116(4):617–28. [PubMed: 14980227]
10. Wei W, Li B, Hanes MA, Kakar S, Chen X, Liu L. S-nitrosylation from GSNOR deficiency impairs DNA repair and promotes hepatocarcinogenesis. Sci Transl Med. 2010; 2(19):19ra13.
11. Wei W, Yang Z, Tang CH, Liu L. Targeted deletion of GSNOR in hepatocytes of mice causes nitrosative inactivation of O6-alkylguanine-DNA alkyltransferase and increased sensitivity to genotoxic diethylnitrosamine. Carcinogenesis. 2011
12. Que LG, Liu L, Yan Y, Whitehead GS, Gavett SH, Schwartz DA, Stamler JS. Protection from experimental asthma by an endogenous bronchodilator. Science. 2005; 308(5728):1618–21. [PubMed: 15919956]
13. Lima B, Lam GK, Xie L, Diesen DL, Villamizar N, Nienaber J, Messina E, Bowles D, Kontos CD, Hare JM, Stamler JS, Rockman HA. Endogenous S-nitrosothiols protect against myocardial injury. Proc Natl Acad Sci U S A. 2009; 106(15):6297–302. [PubMed: 19325130]
14. Whalen EJ, Foster MW, Matsumoto A, Ozawa K, Violin JD, Que LG, Nelson CD, Benhar M, Keys JR, Rockman HA, Koch WJ, Daaka Y, Lefkowitz RJ, Stamler JS. Regulation of beta-adrenergic receptor signaling by S-nitrosylation of G-protein-coupled receptor kinase 2. Cell. 2007; 129(3):511–22. [PubMed: 17482545]
15. Ozawa K, Whalen EJ, Nelson CD, Mu Y, Hess DT, Lefkowitz RJ, Stamler JS. S-nitrosylation of beta-arrestin regulates beta-adrenergic receptor trafficking. Mol Cell. 2008; 31(3):395–405. [PubMed: 18691971]
16. Choudhry S, Que LG, Yang Z, Liu L, Eng C, Kim SO, Kumar G, Thyne S, Chapela R, Rodriguez-Santana JR, Rodriguez-Cintron W, Avila PC, Stamler JS, Burchard EG. GSNO reductase and beta2-adrenergic receptor gene-gene interaction: bronchodilator responsiveness to albuterol. Pharmacogenet Genomics. 2010; 20(6):351–8. [PubMed: 20335826]
17. Sanghani PC, Davis WI, Fears SL, Green SL, Zhai L, Tang Y, Martin E, Bryan NS, Sanghani SP. Kinetic and cellular characterization of novel inhibitors of S-nitrosoglutathione reductase. J Biol Chem. 2009; 284(36):24354–62. [PubMed: 19596685]
18. Eu JP, Liu L, Zeng M, Stamler JS. An apoptotic model for nitrosative stress. Biochemistry. 2000; 39(5):1040–7. [PubMed: 10653649]
19. Pi J, Zhang Q, Woods CG, Wong V, Collins S, Andersen ME. Activation of Nrf2-mediated oxidative stress response in macrophages by hypochlorous acid. Toxicol Appl Pharmacol. 2008; 226(3):236–43. [PubMed: 17980396]
20. Woods CG, Fu J, Xue P, Hou Y, Pluta LJ, Yang L, Zhang Q, Thomas RS, Andersen ME, Pi J. Dose-dependent transitions in Nrf2-mediated adaptive response and related stress responses to hypochlorous acid in mouse macrophages. Toxicol Appl Pharmacol. 2009; 238(1):27–36. [PubMed: 19376150]
21. Stamler JS, Jaraki O, Osborne J, Simon DI, Keaney J, Vita J, Singel D, Valeri CR, Loscalzo J. Nitric oxide circulates in mammalian plasma primarily as an S-nitroso adduct of serum albumin. Proc Natl Acad Sci U S A. 1992; 89(16):7674–7. [PubMed: 1502182]
22. Hart TW. Some observations concerning the S-nitroso and S-phenylsulfonyl derivatives of L-cysteine and glutathione. Tetrahedron Letters. 1985; 26(16):2013–16.
23. Wilm M, Shevchenko A, Houthaeve T, Breit S, Schweigerer L, Fotsis T, Mann M. Femtomole sequencing of proteins from polyacrylamide gels by nano-electrospray mass spectrometry. Nature. 1996; 379(6564):466–9. [PubMed: 8559255]
24. Keller A, Nesvizhskii AI, Kolker E, Aebersold R. Empirical statistical model to estimate the accuracy of peptide identifications made by MS/MS and database search. Anal Chem. 2002; 74(20):5383–92. [PubMed: 12403597]
25. Nesvizhskii AI, Keller A, Kolker E, Aebersold R. A statistical model for identifying proteins by tandem mass spectrometry. Anal Chem. 2003; 75(17):4646–58. [PubMed: 14632076]

26. Nittis T, Guittat L, LeDuc RD, Dao B, Duxin JP, Rohrs H, Townsend RR, Stewart SA. Revealing novel telomere proteins using in vivo cross-linking, tandem affinity purification, and label-free quantitative LC-FTICR-MS. Mol Cell Proteomics. 2010; 9(6):1144–56. [PubMed: 20097687]
27. Weng L, Dai H, Zhan Y, He Y, Stepaniants SB, Bassett DE. Rosetta error model for gene expression analysis. Bioinformatics. 2006; 22(9):1111–21. [PubMed: 16522673]
28. Fu J, Woods CG, Yehuda-Shnaidman E, Zhang Q, Wong V, Collins S, Sun G, Andersen ME, Pi J. Low-level arsenic impairs glucose-stimulated insulin secretion in pancreatic beta cells: involvement of cellular adaptive response to oxidative stress. Environ Health Perspect. 2010; 118(6):864–70. [PubMed: 20100676]
29. Mitchell DA, Erwin PA, Michel T, Marletta MA. S-Nitrosation and regulation of inducible nitric oxide synthase. Biochemistry. 2005; 44(12):4636–47. [PubMed: 15779890]
30. Kelleher ZT, Matsumoto A, Stamler JS, Marshall HE. NOS2 regulation of NF-kappaB by S-nitrosylation of p65. J Biol Chem. 2007; 282(42):30667–72. [PubMed: 17720813]
31. Botelho D, Wall MJ, Vieira DB, Fitzsimmons S, Liu F, Doucette A. Top-down and bottom-up proteomics of SDS-containing solutions following mass-based separation. J Proteome Res. 2010; 9(6):2863–70. [PubMed: 20377267]
32. Hartley JW, Evans LH, Green KY, Naghashfar Z, Macias AR, Zerfas PM, Ward JM. Expression of infectious murine leukemia viruses by RAW264.7 cells, a potential complication for studies with a widely used mouse macrophage cell line. Retrovirology. 2008:51. [PubMed: 18577210]
33. Gabay C, Porter B, Fantuzzi G, Arend WP. Mouse IL-1 receptor antagonist isoforms: complementary DNA cloning and protein expression of intracellular isoform and tissue distribution of secreted and intracellular IL-1 receptor antagonist in vivo. J Immunol. 1997; 159(12):5905–13. [PubMed: 9550387]
34. Tsang AH, Lee YI, Ko HS, Savitt JM, Pletnikova O, Troncoso JC, Dawson VL, Dawson TM, Chung KK. S-nitrosylation of XIAP compromises neuronal survival in Parkinson's disease. Proc Natl Acad Sci U S A. 2009; 106(12):4900–5. [PubMed: 19273858]
35. Chung KK, Thomas B, Li X, Pletnikova O, Troncoso JC, Marsh L, Dawson VL, Dawson TM. S-nitrosylation of parkin regulates ubiquitination and compromises parkin's protective function. Science. 2004; 304(5675):1328–31. [PubMed: 15105460]
36. Yang W, Thompson JW, Wang Z, Wang L, Sheng H, Foster MW, Moseley MA, Paschen W. Analysis of Oxygen/Glucose-Deprivation-Induced Changes in SUMO3 Conjugation Using SILAC-Based Quantitative Proteomics. J Proteome Res. 2011
37. Ryter SW, Tyrrell RM. The heme synthesis and degradation pathways: role in oxidant sensitivity. Heme oxygenase has both pro- and antioxidant properties. Free Radic Biol Med. 2000; 28(2):289–309. [PubMed: 11281297]
38. Bishop A, Marquis JC, Cashman NR, Demple B. Adaptive resistance to nitric oxide in motor neurons. Free Radic Biol Med. 1999; 26(7–8):978–86. [PubMed: 10232842]
39. Son E, Jeong J, Lee J, Jung DY, Cho GJ, Choi WS, Lee MS, Kim SH, Kim IK, Suk K. Sequential induction of heme oxygenase-1 and manganese superoxide dismutase protects cultured astrocytes against nitric oxide. Biochem Pharmacol. 2005; 70(4):590–7. [PubMed: 15993853]
40. Motterlini R, Foresti R, Bassi R, Calabrese V, Clark JE, Green CJ. Endothelial heme oxygenase-1 induction by hypoxia. Modulation by inducible nitric-oxide synthase and S-nitrosothiols. J Biol Chem. 2000; 275(18):13613–20. [PubMed: 10788478]
41. Surh YJ, Kundu JK, Li MH, Na HK, Cha YN. Role of Nrf2-mediated heme oxygenase-1 upregulation in adaptive survival response to nitrosative stress. Arch Pharm Res. 2009; 32(8): 1163–76. [PubMed: 19727608]
42. Liu XM, Peyton KJ, Ensenat D, Wang H, Hannink M, Alam J, Durante W. Nitric oxide stimulates heme oxygenase-1 gene transcription via the Nrf2/ARE complex to promote vascular smooth muscle cell survival. Cardiovasc Res. 2007; 75(2):381–9. [PubMed: 17408602]
43. Li CQ, Kim MY, Godoy LC, Thiantanawat A, Trudel LJ, Wogan GN. Nitric oxide activation of Keap1/Nrf2 signaling in human colon carcinoma cells. Proc Natl Acad Sci U S A. 2009; 106(34): 14547–51. [PubMed: 19706542]
44. Fatma N, Kubo E, Chylack LT Jr, Shinohara T, Akagi Y, Singh DP. LEDGF regulation of alcohol and aldehyde dehydrogenases in lens epithelial cells: stimulation of retinoic acid production and

protection from ethanol toxicity. Am J Physiol Cell Physiol. 2004; 287(2):C508–16. [PubMed: 15238362]

45. Fatma N, Singh DP, Shinohara T, Chylack LT Jr. Transcriptional regulation of the antioxidant protein 2 gene, a thiol-specific antioxidant, by lens epithelium-derived growth factor to protect cells from oxidative stress. J Biol Chem. 2001; 276(52):48899–907. [PubMed: 11677226]
46. Bateman RL, Rauh D, Tavshanjian B, Shokat KM. Human carbonyl reductase 1 is an S-nitrosoglutathione reductase. J Biol Chem. 2008; 283(51):35756–62. [PubMed: 18826943]
47. Potter AJ, Kidd SP, Edwards JL, Falsetta ML, Apicella MA, Jennings MP, McEwan AG. Esterase D is essential for protection of Neisseria gonorrhoeae against nitrosative stress and for bacterial growth during interaction with cervical epithelial cells. J Infect Dis. 2009; 200(2):273–8. [PubMed: 19527171]
48. Nguyen TT, Hu Y, Widney DP, Mar RA, Smith JB. Murine GBP-5, a new member of the murine guanylate-binding protein family, is coordinately regulated with other GBPs in vivo and in vitro. J Interferon Cytokine Res. 2002; 22(8):899–909. [PubMed: 12396730]
49. Nicolet CM, Paulnock DM. Promoter analysis of an interferon-inducible gene associated with macrophage activation. J Immunol. 1994; 152(1):153–62. [PubMed: 8254188]
50. MacMicking JD. IFN-inducible GTPases and immunity to intracellular pathogens. Trends Immunol. 2004; 25(11):601–9. [PubMed: 15489189]
51. Kim BH, Shenoy AR, Kumar P, Das R, Tiwari S, MacMicking JD. A family of IFN-gamma-inducible 65-kD GTPases protects against bacterial infection. Science. 2011; 332(6030):717–21. [PubMed: 21551061]
52. Rodriguez-Pascual F, Hausding M, Ihrig-Biedert I, Furneaux H, Levy AP, Forstermann U, Kleinert H. Complex contribution of the 3′-untranslated region to the expressional regulation of the human inducible nitric-oxide synthase gene. Involvement of the RNA-binding protein HuR. J Biol Chem. 2000; 275(34):26040–9. [PubMed: 10859327]
53. Soderberg M, Raffalli-Mathieu F, Lang MA. Identification of a regulatory cis-element within the 3′-untranslated region of the murine inducible nitric oxide synthase (iNOS) mRNA, interaction with heterogeneous nuclear ribonucleoproteins I and L and role in the iNOS gene expression. Mol Immunol. 2007; 44(4):434–42. [PubMed: 16584775]
54. Sumi D, Ignarro LJ. Regulation of inducible nitric oxide synthase expression in advanced glycation end product-stimulated raw 264. 7 cells: the role of heme oxygenase-1 and endogenous nitric oxide. Diabetes. 2004; 53(7):1841–50. [PubMed: 15220209]
55. Lee SH, Seo GS, Ko G, Kim JB, Sohn DH. Anti-inflammatory activity of 20(S)-protopanaxadiol: enhanced heme oxygenase 1 expression in RAW 264. 7 cells. Planta Med. 2005; 71(12):1167–70. [PubMed: 16395656]
56. Chen TH, Hsu YT, Chen CH, Kao SH, Lee HM. Tanshinone IIA from Salvia miltiorrhiza induces heme oxygenase-1 expression and inhibits lipopolysaccharide-induced nitric oxide expression in RAW 264. 7 cells. Mitochondrion. 2007; 7(1–2):101–5. [PubMed: 17300995]
57. Tsoyi K, Kim HJ, Shin JS, Kim DH, Cho HJ, Lee SS, Ahn SK, Yun-Choi HS, Lee JH, Seo HG, Chang KC. HO-1 and JAK-2/STAT-1 signals are involved in preferential inhibition of iNOS over COX-2 gene expression by newly synthesized tetrahydroisoquinoline alkaloid, CKD712, in cells activated with lipopolysacchride. Cell Signal. 2008; 20(10):1839–47. [PubMed: 18634870]
58. Sun X, Qiu J, Strong SA, Green LS, Wasley JW, Colagiovanni DB, Mutka SC, Blonder JP, Stout AM, Richards JP, Chun L, Rosenthal GJ. Structure-activity relationships of pyrrole based S-nitrosoglutathione reductase inhibitors: Pyrrole regioisomers and propionic acid replacement. Bioorg Med Chem Lett. 2011; 21(12):3671–5. [PubMed: 21570838]
59. Sun X, Wasley JWF, Qiu J, Blonder JP, Stout AM, Green LS, Strong SA, Colagiovanni DB, Richards JP, Mutka SC, Chun L, Rosenthal GJ. Discovery of S-Nitrosoglutathione Reductase Inhibitors: Potential Agents for the Treatment of Asthma and Other Inflammatory Diseases. ACS Medicinal Chemistry Letters. 2011; 2(5):402–406.
60. Donnelly LE, Barnes PJ. Expression of heme oxygenase in human airway epithelial cells. Am J Respir Cell Mol Biol. 2001; 24(3):295–303. [PubMed: 11245628]

61. Srisook K, Cha YN. Super-induction of HO-1 in macrophages stimulated with lipopolysaccharide by prior depletion of glutathione decreases iNOS expression and NO production. Nitric Oxide. 2005; 12(2):70–9. [PubMed: 15740980]
62. Wang P, Liu GH, Wu K, Qu J, Huang B, Zhang X, Zhou X, Gerace L, Chen C. Repression of classical nuclear export by S-nitrosylation of CRM1. J Cell Sci. 2009; 122(Pt 20):3772–9. [PubMed: 19812309]
63. Kuwano Y, Rabinovic A, Srikantan S, Gorospe M, Demple B. Analysis of nitric oxide-stabilized mRNAs in human fibroblasts reveals HuR-dependent heme oxygenase 1 upregulation. Mol Cell Biol. 2009; 29(10):2622–35. [PubMed: 19289500]
64. Chang CL, Au LC, Huang SW, Fai Kwok C, Ho LT, Juan CC. Insulin up-regulates heme oxygenase-1 expression in 3T3-L1 adipocytes via PI3-kinase- and PKC-dependent pathways and heme oxygenase-1-associated microRNA downregulation. Endocrinology. 2011; 152(2):384–93. [PubMed: 21147878]
65. Zhang H, Forman HJ. Acrolein induces heme oxygenase-1 through PKC-delta and PI3K in human bronchial epithelial cells. Am J Respir Cell Mol Biol. 2008; 38(4):483–90. [PubMed: 18048804]
66. Rushworth SA, Chen XL, Mackman N, Ogborne RM, O'Connell MA. Lipopolysaccharide-induced heme oxygenase-1 expression in human monocytic cells is mediated via Nrf2 and protein kinase C. J Immunol. 2005; 175(7):4408–15. [PubMed: 16177082]
67. Chen L, Kong X, Fu J, Xu Y, Fang S, Hua P, Luo L, Yin Z. CHIP facilitates ubiquitination of inducible nitric oxide synthase and promotes its proteasomal degradation. Cell Immunol. 2009; 258(1):38–43. [PubMed: 19362296]
68. Kuang Z, Lewis RS, Curtis JM, Zhan Y, Saunders BM, Babon JJ, Kolesnik TB, Low A, Masters SL, Willson TA, Kedzierski L, Yao S, Handman E, Norton RS, Nicholson SE. The SPRY domain-containing SOCS box protein SPSB2 targets iNOS for proteasomal degradation. J Cell Biol. 2010; 190(1):129–41. [PubMed: 20603330]
69. Nishiya T, Matsumoto K, Maekawa S, Kajita E, Horinouchi T, Fujimuro M, Ogasawara K, Uehara T, Miwa S. Regulation of inducible nitric-oxide synthase by the SPRY domain- and SOCS box-containing proteins. J Biol Chem. 2011; 286(11):9009–19. [PubMed: 21199876]
70. Yao D, Gu Z, Nakamura T, Shi ZQ, Ma Y, Gaston B, Palmer LA, Rockenstein EM, Zhang Z, Masliah E, Uehara T, Lipton SA. Nitrosative stress linked to sporadic Parkinson's disease: S-nitrosylation of parkin regulates its E3 ubiquitin ligase activity. Proc Natl Acad Sci U S A. 2004; 101(29):10810–4. [PubMed: 15252205]
71. Diet A, Abbas K, Bouton C, Guillon B, Tomasello F, Fourquet S, Toledano MB, Drapier JC. Regulation of peroxiredoxins by nitric oxide in immunostimulated macrophages. J Biol Chem. 2007; 282(50):36199–205. [PubMed: 17921138]
72. Wegiel B, Gallo D, Csizmadia E, Roger T, Kaczmarek E, Harris C, Zuckerbraun BS, Otterbein LE. Biliverdin inhibits Toll-like receptor-4 (TLR4) expression through nitric oxide-dependent nuclear translocation of biliverdin reductase. Proc Natl Acad Sci U S A. 2011; 108(46):18849–18854. [PubMed: 22042868]

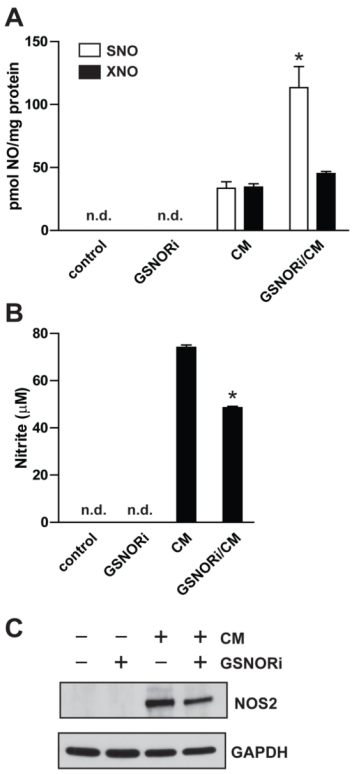

Figure 1.

Quantification of NO-derived species and NOS2 expression in cytokine-stimulated and GSNORi-treated RAW 264.7 mouse macrophages. RAW 264.7 cells were pretreated with GSNORi for 30 min followed by 0.5 μg/ml LPS and 10 ng/ml IFN-γ (cytomix; CM) for 16 h. (A) High-mass (i.e. protein-bound) NO was quantified by photolysis chemiluminescence analysis. SNO and XNO species were discriminated by displacement of SNO with Hg(II)[8]. (B) Nitrite was measured in culture media by Griess assay. (C) NOS2 expression was measured in cell lysates by western blotting. Data in A and B are mean ± S.E.M. (n=3), *$p<0.05$ versus CM, unpaired t-test.

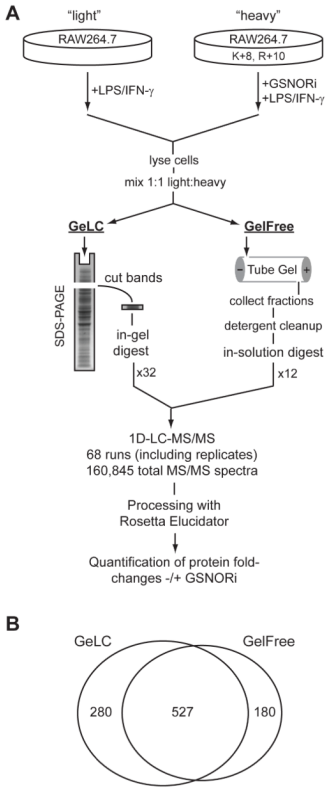

Figure 2.

Quantitative analysis of protein expression in RAW 264.7 treated ± GSNORi. (A) Schematic of SILAC methodology, using SDS-PAGE-based (GeLC) and GelFree fractionation. (B) Venn diagram showing number of proteins quantified by GeLC and GelFree analysis and overlap between the two datasets.

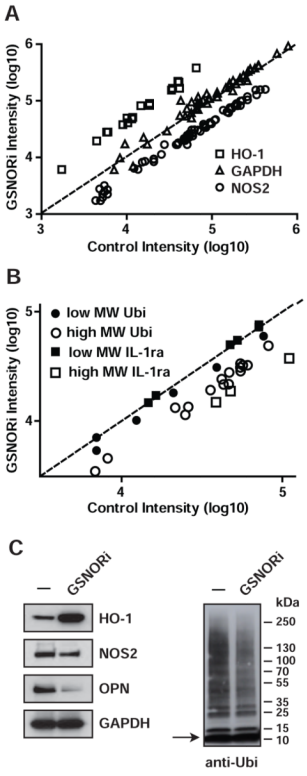

Figure 3.

Exemplary peptide-level quantitation and validation of proteomic data. (A) Plot of heavy (+GSNORi) versus light (control) peptide intensities for SILAC pairs of GAPDH (51 pairs), HO-1 (18 pairs), NOS2 (70 pairs). Data was from GeLC analysis and includes redundant pairs identified in multiple fractions or having multiple charge states. Average fold changes were +1.2 for GAPDH, −2.3 for NOS2 and +4.6 for HO-1. (B) Plot of heavy (+GSNORi) versus light (control) peptide intensities for SILAC pairs of ubiquitin (Ubi) and interleukin 1 receptor antagonist (IL-1ra) from GeLC analysis. For Ubi, low MW data was from gel band 32 and high MW data was from gel bands 2–9. For IL-1ra, low MW data was from gel band 30 and high MW data was from gel band 29. (C-D) Western blotting was performed on lysates from cytokine-stimulated RAW 264.7 cells that were untreated (-) or treated with GSNORi. Low-mass ubiquitin in (D) is indicated by arrow.

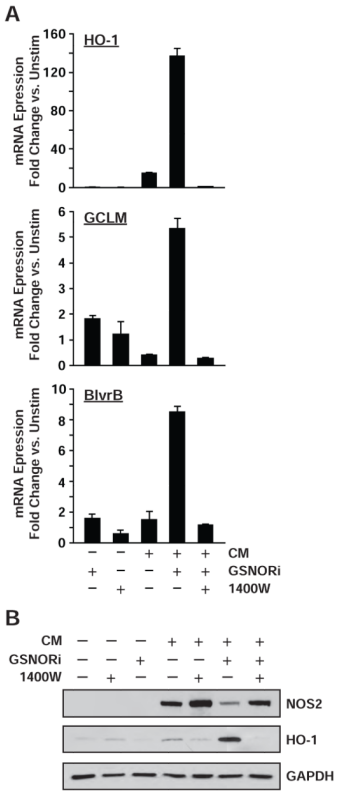

Figure 4.

Transcriptional and NOS2-dependent effects of GSNORi. (A) RT-PCR was performed on RAW 264.7 cells stimulated for 16 h with CM, 50 μM GSNORi, 100 μM 1400W or combinations thereof. Data was normalized to actin. (B) Western blotting was performed on RAW 264.7 cells treated as in A. Data in A are mean ± range from two replicates and data in B are representative of 3 independent experiments.

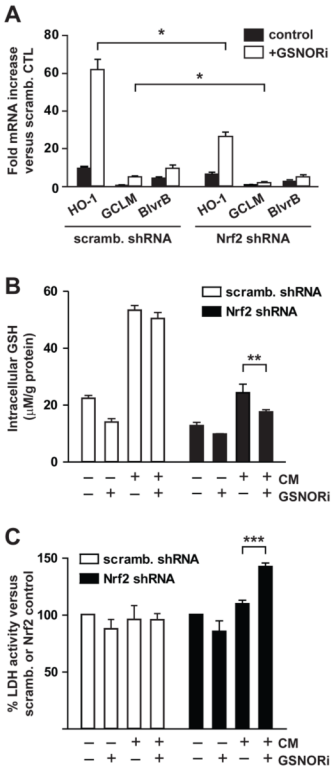

Figure 5.

Effects of Nrf2 knockdown on GSNORi-mediated gene expression and nitrosative stress resistance. RAW 264.7 cells stably expressing scrambled versus Nrf2 shRNA were treated ± CM and ± GSNORi for 16 h. (A) mRNA expression was measured by RT-PCR (B) GSH concentrations were assayed in cell lysates. (C) LDH activity was assayed in cell culture supernatants. Data in A-C are mean ± S.E.M (n=3 per group). *p<0.005 versus scramb. shRNA; **p<0.05 versus CM; ***p<0.01 versus CM (unpaired t-test).

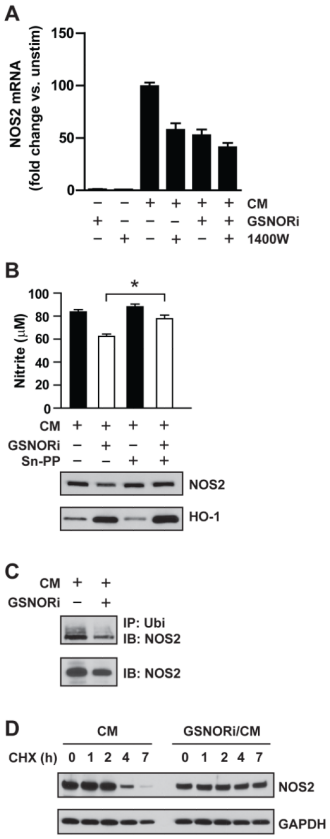

Figure 6.

Mechanisms of NOS2 downregulation by GSNORi. (A) mRNA expression was measured in RAW 264.7 cells treated for 16 h ± CM, 50 μM GSNORi and 100 μM 1400W. (B) RAW cells were treated ± 2.5 μM tin protoporphyrin IX (Sn-PP) and 50 μM GSNORi, and stimulated overnight with cytomix. Nitrite in cell culture supernatants was analyzed by Griess assay, and lysates were probed by western blotting. (C), Polyubiquitinated proteins were precipitated with TUBE1-agarose from lysates of RAW 264.7 cells were treated with CM ± 50 μM GSNORi for 16 h. Immunoprecipitates were eluted by boiling in loading buffer, and western blotting was performed. (D) RAW 264.7 cells were treated as in (C) for 16 h followed by addition of 100 μM cyclohexamide (CHX). Lysates were harvested at the indicated time and analyzed by western blotting. Data in A and B are mean ± S.E.M (n=3). *$p<0.02$ (unpaired t-test).

Table 1

Proteins induced by GSNORi in cytokine-stimulated RAW 264.7 cells. Proteins were selected based on fold-change >1.3, 2+ SILAC pairs and p<0.001. Proteins that were common to both GeLC and GelFree data were included only if they exhibited similar fold changes. See Supporting Information for complete datasets.

		GeLC			GelFree		
Protein Name	**Protein Description**	**Fold Change**	**p-value**	**#SILAC pairs**	**Fold Change**	**p-value**	**#SILAC Pairs**
HMOX1_MOUSE	Heme oxygenase 1	4.6	<1.0E-8	12	3.8	<1.0E-8	3
GSH0_MOUSE	Glutamate-cysteine ligase modulatory subunit	-	-	-	1.9	<1.0E-8	2
ICAM1_MOUSE	Intracellular adhesion molecule 1	-	-	-	1.6	<1.0E-8	8
GBP4_MOUSE	Guanylate-binding protein 4	1.5	<1.0E-8	4	-	-	-
GBP5_MOUSE	Guanylate-binding protein 5	1.5	<1.0E-8	5	1.6	7.5E-7	2
PSIP1_MOUSE	Lens epithelial-derived growth factor	1.5	1.9E-7	2	-	-	-
NIBAN_MOUSE	Protein Niban	1.4	<1.0E-8	3	-	-	-
BLVRB_MOUSE	Biliverdin reductase B	1.4	4.9E-7	4	1.3	2.1E-8	3
THIC_MOUSE	Acetyl-CoA acetyltransferase, cytosolic	1.4	<1.0E-8	2	-	-	-
CNPY2_MOUSE	Protein canopy homolog 2	-	-	-	1.4	1.8E-7	5
LGUL_MOUSE	Lactoylglutathione lyase	1.4	0.001	2	-	-	-
ALD2_MOUSE	Aldose reductase-related protein 2 (Akr1b8)	1.4	5.3E-5	4	1.4	0.002	4
SLK_MOUSE	STE20-like serine/threonine-protein kinase	1.4	<1.0E-8	2	-	-	-
GBP1_MOUSE	Guanylate-binding protein 1	1.3	<1.0E-8	7	1.3	<1.0E-8	5

Table 2

Proteins downregulated by GSNORi in cytokine-stimulated RAW 264.7 cells. Proteins were selected based on fold-change <1.5, 2+ SILAC pairs and p<0.001. Proteins that were common to both GeLC and GelFree data were included only if they exhibited similar fold changes. See Supporting Information for complete datasets.

		GeLC			GelFree		
Protein Name	**Protein Description**	**Fold Change**	**p-value**	**#SILAC pairs**	**Fold Change**	**p-value**	**#SILAC Pairs**
OSTP_MOUSE	Osteopontin	-	-	-	−2.9	<1.0E-8	4
ENV_MLVMO	Envelope glycoprotein	−2.6	<1.0E-8	4	-	-	-
CQ087_MOUSE	Transmembrane protein C17orf87 homolog	-	-	-	−2.4	1.6E-4	2
BASP_MOUSE	Brain acid soluble protein 1	−2.4	<1.0E-8	3	−2.1	<1.0E-8	5
NOS2_MOUSE	Nitric oxide synthase, inducible	−2.3	<1.0E-8	43	−1.9	0.007	2
RSAD2_MOUSE	Radical S-adenosyl methionine domain-containing protein 2	−2.1	<1.0E-8	4	−2.0	<1.0E-8	3
STX12_MOUSE	Syntaxin-12	−2.0	2.5E-4	2	-	-	-
MPEG1_MOUSE	Macrophage-expressed gene 1 protein	-	-	-	−1.9	4.7E-5	3
UPP1_MOUSE	Uridine phosphorylase 1	−1.8	<1.0E-8	3	-	-	-
PCKGM_MOUSE	Phosphoenolpyruvate carboxykinase [GTP], mitochondrial	−1.8	<1.0E-8	3	-	-	-
TXNL1_MOUSE	Thioredoxin-like protein 1	−1.8	<1.0E-8	3	−1.6	1.1E-8	4
MAOM_MOUSE	NAD-dependent malic enzyme, mitochondrial	−1.8	2.6E-8	4	-	-	-
HXK1_MOUSE	Hexokinase-1	−1.7	<1.0E-8	6	−1.5	<1.0E-8	4
SF3A3_MOUSE	Splicing factor 3A subunit 3	−1.7	2.2E-4	2	-	-	-
ODPB_MOUSE	Pyruvate dehydrogenase E1 component subunit beta	−1.7	8.3E-4	6	−1.4	<1.0E-8	4
LAMP2_MOUSE	Lysosome-associated membrane glycoprotein 2	−1.7	<1.0E-8	4	-	-	-
F162A_MOUSE	UPF0389 protein FAM162A	-	-	-	−1.6	7.6E-4	2
MATR3_MOUSE	Matrin-3	−1.6	5.2E-6	2	-	-	-
FCERG_MOUSE	High affinity immunoglobulin epsilon receptor subunit gamma	−1.6	<1.0E-8	3	−1.4	<1.0E-8	3
HNRPL_MOUSE	Heterogeneous nuclear ribonucleoprotein L	−1.6	<1.0E-8	5	−1.4	0.008	5
CMC1_MOUSE	Calcium-binding mitochondrial carrier protein	−1.5	1.8E-4	3	−1.4	4.8E-4	3
TM38B_MOUSE	Trimeric intracellular cation channel type B	−1.5	3.0E-7	3	-	-	-
PGH2_MOUSE	Prostaglandin G/H synthase 2	−1.5	<1.0E-8	22	−1.4	<1.0E-8	40